Thiol-ene emulsion step polymerization in a photochemical stirred tank reactor: Molecular weight, cyclization, and fragmentation

Cuong Minh Quoc Le, Abraham Chemtob

Received: 16 July 2022 | Revised: 26 September 2022 | Accepted: 5 October 2022

DOI: 10.1002/pol.20220402

RESEARCH ARTICLE

JOURNAL OF POLYMER SCIENCE WILEY

Thiol-ene emulsion step polymerization in a photochemical stirred tank reactor: Molecular weight, cyclization, and fragmentation

Cuong Minh Quoc Le[1,2] | **Abraham Chemtob**[1,2]

[1]Université de Haute-Alsace, CNRS, IS2M UMR7361, Mulhouse, France

[2]Université de Strasbourg, France

Correspondence
Abraham Chemtob, Université de Haute-Alsace, CNRS IS2M UMR7361, F-68100 Mulhouse, France.
Email: abraham.chemtob@uha.fr

Funding information
H2020 Excellent Science, Grant/Award Number: 765341; European Union; Horizon 2020

Abstract

Unlike many step polymerizations, the polymerization of bifunctional thiol and alkene monomers can be carried in emulsion to prepare a range of sulfur-containing polymer particles differing markedly from conventional emulsion chain polymers. This study examines how the change of polymerization mechanism affects polymer molecular weight, structure and composition. A 2,2′-dimercaptodiethyl sulfide/diallyl phthalate emulsion is photopolymerized in a photochemical stirred-tank reactor equipped with Light-emitting diodes (LEDs) to yield a 30% solids content latex with a high weight-average molecular weight (100 kDa) and a broad molecular weight distribution ($Đ = 8.5$). Intramolecular cyclization occurs during polymerization by the addition of a thiyl radical to the unsaturated end group of the same molecule. Irreversible ring-closure takes place to produce "dead" cyclic oligomers in the early stage of the reaction, whereas chain-growth continues at high conversion. Consequently, the particles are composed of high molecular weight linear chains and a fraction of stable oligomer cycles, showing a broad and bimodal molecular weight distribution. The linear poly(thioether) chains include occasionally disulfide units due to thiyl radical recombination. The reversibility of disulfide bonds causes a decrease of molecular weight during storage. The addition of radical inhibitor to the latex stops fragmentation of SS bonds.

KEYWORDS

emulsion polymerization, photopolymerization, photoreactor, step polymerization

1 | INTRODUCTION

Most emulsion polymerizations proceed via free or controlled radical chain polymerization mechanism, which has the advantage of being tolerant toward water.[1] Unlike chain polymerizations, the kinetic and thermodynamic feasibility of many conventional step polymerizations are severely decreased by the presence of water, to such an extent that their handling in emulsion is generally deemed impractical or impossible.[2] Firstly, water precludes the use of high temperatures (>150 °C) generally needed to obtain reasonable polymerization rates and high conversions. Secondly, the stoichiometry may be lost by undesirable side reactions between the

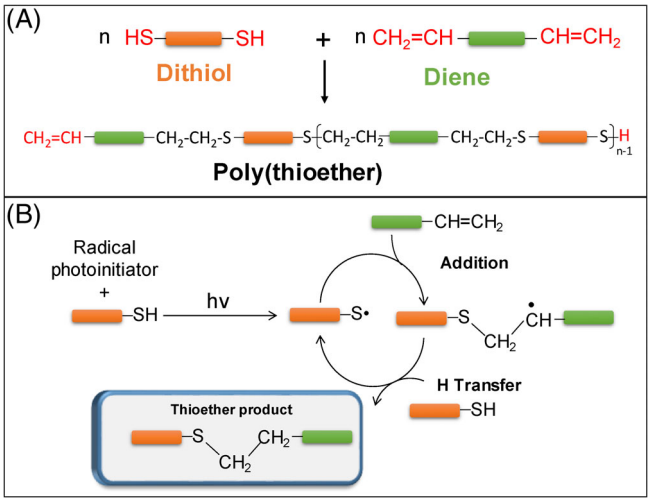

SCHEME 1 (A). Radical-mediated thiol-ene step polymerization involving bifunctional monomers. (B) Mechanism of radical-mediated thiol-ene reaction

monomers and water (e.g., polyurethane). Thirdly, step polymerizations are often equilibrium reactions involving water as by-product (e.g., polyesterification), therefore, hence, driving the equilibrium toward polymer is impossible to achieve when the polymerization occurs in emulsion. Literature data show that rare cases of emulsion step polymerizations generally stop short of completion, resulting in latexes containing mainly low molecular weight (MW) species.[2–5]

Interestingly, the radical-mediated polyaddition of dithiol with diene linear monomers (Scheme 1A) is an exception to this generalization since high MW poly (thioether) colloidal dispersions have been recently achieved by emulsion polymerization, but with low solids content (10 wt%).[6–8] To date, much of the interest in thiol-ene polymerization has been on cross-linked structures obtained under UV irradiation and bulk conditions to produce coatings, printing inks and 3D printed objects.[9–11] In contrast, linear polymer particles dispersed in water (latex) are produced in emulsion thiol-ene polymerization, paving the way to other products and applications. In this case, the water-insoluble thiol and ene monomers are dispersed in water by means of a surfactant used at a concentration exceeding its critical micelle concentration (CMC). The polymerization is initiated by a water-soluble radical (photo)initiator, whose decomposition forms primary radicals that subsequently abstract hydrogen from thiols to yield thiyl radicals. These latter species then initiate a step polymerization consisting of alternating radical addition and chain transfer reactions (Scheme 1B). Unlike other step polymerizations, the formation of high polymers is made possible by distinct characteristic features of the thiol-ene chemistry:[12] the absence of by-products, high polymerization rates at ambient temperature (for a wide range of monomers) and a water-insensitive radical-mediated polymerization mechanism.[13] The first investigations showed that the number of polymer particles formed and the nucleation mechanism did not deviate significantly from the normal chain pathway.[14] By contrast, significantly different behaviors are expected regarding polymer MW (evolution throughout the reaction and distribution) and structures (linear, branched, cross-linked and cyclic products), for which very few data are currently available.[15]

In contrast to chain polymerization,[16] linear step polymerization is characterized by the difficulty to obtain high MW polymers, which are formed only late in the reaction that is, at very high overall monomer conversions (>98%–99%).[16] In addition, the parameters and phenomena controlling the width of MW distributions are different for the two polymerization mechanisms. For chain polymerization, it is established that the MW distributions are generally broad at high conversions, especially when chain transfer to the polymer takes place.[17] The occurrence of this latter reaction gives rise to branched and cross-linked structures in addition to linear chains. Conversely, chain transfer to the polymer is negligible in thiol-ene step polymerization because chain transfer to thiols, as an integral part of the propagation mechanism, has a much higher rate constant. Therefore, branching and cross-linking are highly unlikely when bifunctional thiol and ene monomers are used. However, cyclic species may form depending on reaction conditions and ring strain, as described in a number of step polymerizations.[18] Therefore, the typical step polymer contains predominantly linear species and a varying amount of cyclic species.[19] Bimodal MW distributions are usually observed in these polymerizations because the cycles are mainly oligomers whereas the linear chains have high MW.[20]

We report a comprehensive study of the polymer MW, structure and composition during the step photopolymerization of an emulsion based on 2,2′-dimercaptodiethyl sulfide (DMDS) and diallyl phthalate (DAP) (Scheme 2). The photochemical reactor and the ratio of monomers to water were chosen to be consistent with the conditions of conventional emulsion chain polymerizations.[21] Thus, a standard monomer phase content of approximately 30 wt% was chosen to yield eventually high solids content latexes. We also designed a novel stirred tank photochemical reactor composed of a 500 ml glass vessel fitted with an overhead stirrer and surrounded by eight LED vertical modules (385 nm) adjustable in their position in order to vary the irradiance (Figure 1).[22] The experimental conditions (initiator concentration, solids content) favorable for the formation of high MW polymers are described in the

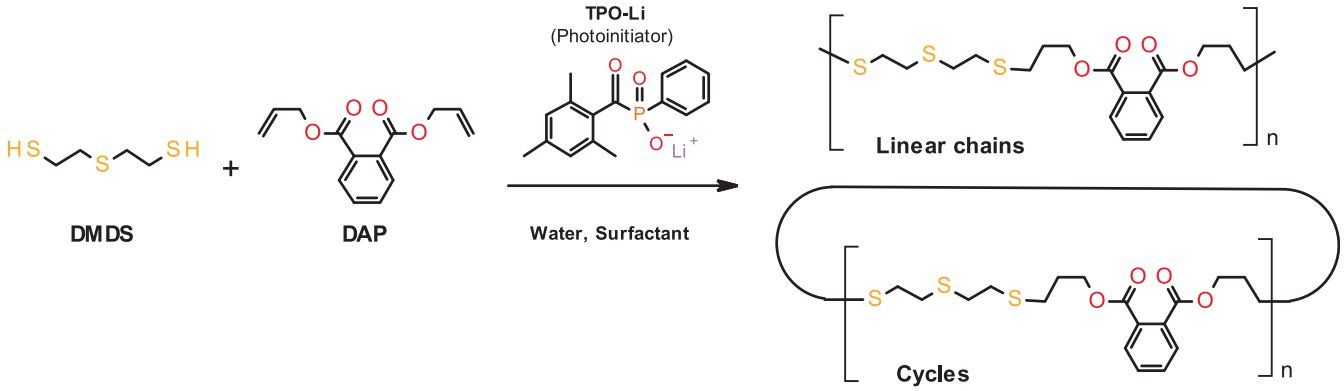

SCHEME 2 Step polymerization of 2,2′-dimercaptodiethyl sulfide (DMDS) with diallyl phthalate (DAP). The monomers can undergo linear polymerization or irreversible intramolecular cyclization

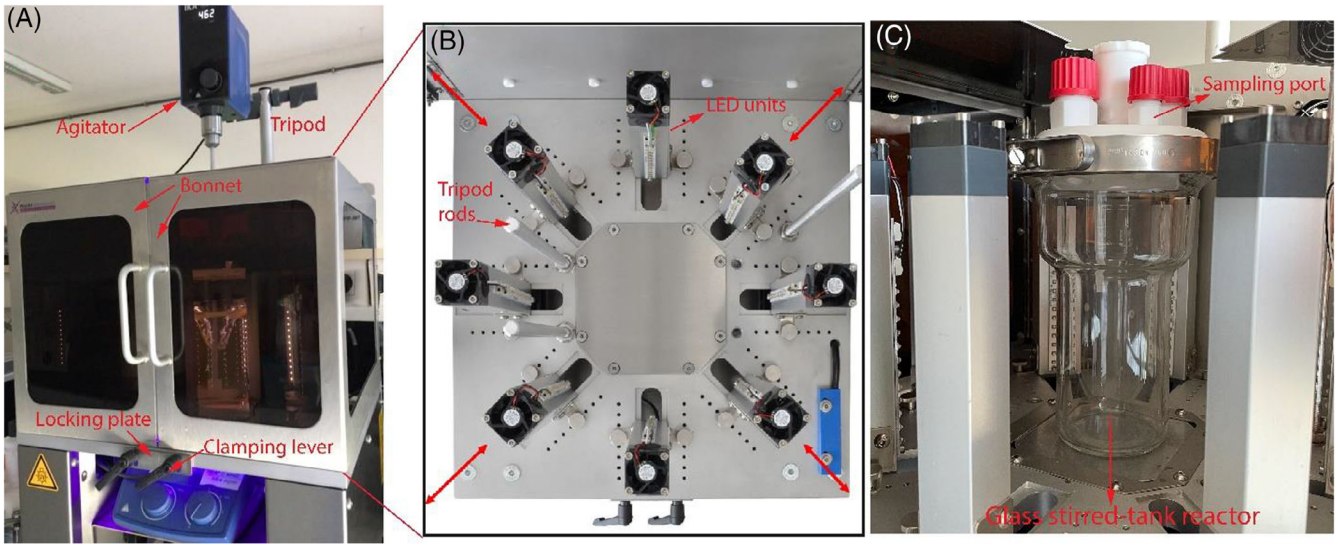

FIGURE 1 (A) Photochemical reactor platform designed by Peschl Ultraviolet GmbH consisting of a stainless steel/aluminum housing with two UV protective service doors, a head agitator and a magnetic drive. (B) The housing accommodates eight air-cooled 385 nm LED-units (24 W each). (C) A 500 ml cylindrical stirred-tank reactor used to perform emulsion thiol-ene polymerization

Section 3.4. For reasons of practicability and clarity, our study does not involve other monomers than DMDS and DAP.

2 | EXPERIMENTAL SECTION

2.1 | Materials

Diallyl phthalate (DAP, TCI, 99.1%), 2,2′-dimercaptodiethyl sulfide (DMDS, Bruno Bock, 98.7%), sodium dodecyl sulfate (SDS, TCI 98%), tributylphosphine (Aldrich, mixture of isomers 98.4%), pyrogallol (TCI, 99%), ethyl phenyl(2,4,6-trimethylbenzoyl)phosphinate (Speedcure TPO-L, Lamson Ltd UK, ≥94.5%), LiBr (TCI, >99%), butan-2-one (TCI, for spectroscopy >99%), petroleum ether (ROTH, 40–60 °C), were used as received. DMSO-d^6 (99.8% D), $CDCl_3$ (99.8% D), D_2O (99.9% D) were purchased from Eurisotop.

2.2 | Synthesis

2.2.1 | Synthesis of lithium phenyl (2,4,6-trimethylbenzoyl)phosphinate

The water-soluble radical photoinitiator lithium phenyl (2,4,6-trimethylbenzoyl)phosphinate (TPO-Li) was synthesized according to the procedure published by Majima et al.[23] 10.75 g of Speedcure TPO-L (32.1 mmol, 1 eq.) were dissolved in 150 ml of butan-2-one, then 11.81 g of LiBr (134.6 mmol, 4.2 eq.) were added and the resulting

solution was stirred vigorously at room temperature for 15 min. The mixture was then heated to 65°C and stirred for 2 h. The resulting yellow precipitate was filtered off and washed with butan-2-one and petroleum ether (2 × 50 ml). The final product was dried under vacuum to yield TPO-Li (7.8 g, 83%) as a white powder. ^{1}H nuclear magnetic resonance (NMR) (300 MHz, D_2O) δ 7.62 (dd, 2H), 7.51–7.41 (m, 1H), 7.36 (td, 2H), 6.77 (s, 2H), 2.12 (s, 3H), 1.92 (s, 6H).

2.3 | Emulsion thiol-ene polymerization in a batch photochemical stirred tank reactor

One hundred and sixty grams of organic thiol-ene phase was prepared by mixing stoichiometric amounts of 98.25 g of DAP (0.395 mol) and 61.8 g of DMDS (0.395 mol). An aqueous phase was prepared separately by adding 0.400 g of TPO-Li (1.34 mmol, 3.73 mM/water) and 3.18 g of SDS (10.81 mmol or 30 mM in water) to 360.0 ml of deionized water. The organic and aqueous phases were added to a 500 ml stirred tank reactor (Figure 1C), mixed under magnetic stirring (15,000 rpm) for 10 min, then emulsified with an Ultra-Turrax mixer (T25 digital-IKA, dispersing tool: 18 mm dispersing tool S25N-18G). Photopolymerization was performed at room temperature immediately after emulsification by placing the reactor at the center of MDPS® batch photochemical reactor platform designed by Peschl Ultraviolet GmbH (Figure 1A). The photochemical equipment consists of a stainless steel/aluminum housing with two service doors, two housing fans as well as eight air-cooled 385 nm LED-units surrounding the reactor (Figure 1B). Each LED-unit is consists of 12 individual LEDs (2 W each), resulting in a total power consumption of 24 W per LED-unit. All LEDs can be dimmed from 10% to 100% (see the evolution of irradiance at the reactor surface depending on the power in Figure S1) and are equipped with a temperature sensor. The irradiation was controlled via a power supply unit. Unless otherwise mentioned, the irradiance at the surface of the reactor was 32.8 mW cm^{-2} (100% power). A continuous reactor stirring at 1100 rpm was ensured during the polymerization by either an integrated IKA head agitator (MINISTAR 20 digital—MINI-ST 20D) or magnetic drive (RCT basic 620 W) placed on the mobile platform beneath the reactor. The reactor is covered with a removable UV shield controlled by a reed contact switch for safe operation. Unless otherwise stated, photochemical experiments were carried at room temperature (21–22°C) with a time of irradiation of 1 h and a stirring speed of 1500 rpm. A digital thermometer (TP3001, LABBOX—50–300°C, resolution 0.1°C) was inserted into the reactor to monitor the temperature rise during the reaction. One milliliter aliquots were taken from the reaction system at different irradiation times, for subsequent analysis of monomer conversion, particle size, and MW.

2.4 | Characterization

2.4.1 | Nuclear magnetic resonance

The double bond conversion during the course of the reaction was determined by ^{1}H-NMR in DMSO-d^6. A portion of 30 µl aliquot was dissolved in 570 µl DMSO-d^6. The integral of the methylene protons 4.7 and 4.25 ppm in monomer and polymer, respectively, was used to determine the conversion. For DMSO-insoluble samples (high conversion), 100 µl of latex were precipitated in 500 µl of saturated sodium chloride solution and washed twice with water. The solid polymer was dried under vacuum before being dissolved in $CDCl_3$ for 1H-NMR analysis. All NMR spectra were recorded using a Varian 300—MR. All chemical shifts were reported in parts per million (ppm) relative to the residual DMSO-d^6 (δ 2.50 ppm). At least 64 scans were acquired for each spectrum.

2.4.2 | Size exclusion chromatography

MW were determined using an Agilent 1260 infinity size exclusion chromatography (SEC) equipped with a G1314B variable UV detector operating at 280 nm, a G7800A multidetector suite consisting of a refractive index detector and a viscosity detector. THF was used as an eluent. The solution was pumped through a set of columns (Polymer Laboratories ResiPore, nominal particle size: 3 µm; porosity: 2 µm) consisting of one guard column (50 × 7.5 mm) and two columns (300 × 7.5 mm). The flow rate was set to 1 ml min^{-1} and the column temperature was controlled at 35°C. The system was then calibrated using calibration standards (EasiVial polystyrene standards from Agilent) ranging from 162 to 591,000 Da. A 15 µl latex sample was weighed in a four-digit balance before being dissolved in 1.5 ml of THF. The polymer solution was filtered through a 0.2 µm PTFE membrane before injection. Agilent GPC/SEC software and multi-detector were used to obtain the molecular weight data. Note that the calculation of MW was started at a mass around 300 Da, to include all oligomers. For a detailed description of the MW calculation, see Figure S2. To study chain fragmentation and its effect on polymer MW, 15 µl of tributylphosphine (known as an efficient —S—S— reducing agent) were added to the vial

containing the filtered polymer solution used for SEC. The solution was re-injected after standing at room temperature for 1 h.

2.4.3 | Dynamic light scattering

Particle sizes were determined by dynamic light scattering (DLS) (VASCO particle size analyzer-Cordouan technologies) with a laser source of 658 nm and a detector set to a scattering angle of 135°. The latexes were diluted in deionized water prior to measurement to achieve a solids content of 0.1%. The diluted sample was transferred to the DLS cell, and the Dual Thickness Controller (DTC) was set to DOWN. Each sample was analyzed 10 times in statistical mode with a signal to noise limit of 1%. The z-average diameters were computed by NanoQ software version 2.6 using the cumulant data analysis mode.

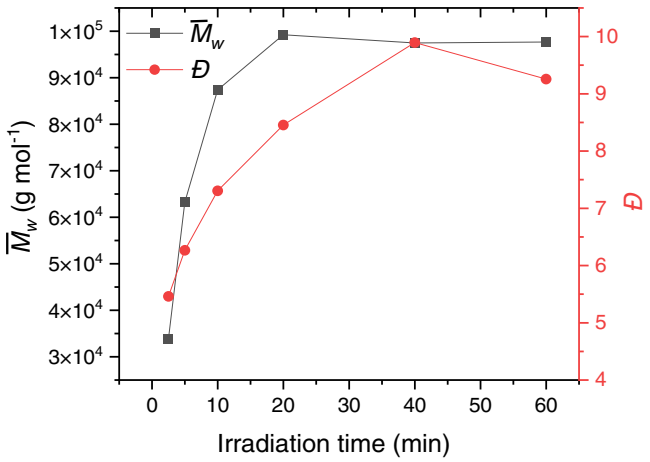

FIGURE 2 Weight-average MW and MW dispersity ($Đ$) evolution in the emulsion photopolymerization of diallyl phthalate-2,2′-dimercaptodiethyl sulfide. Monomer content = 30.8%w (TPO-Li) = 3.73 mM/water, and (SDS) = 30 mM/water, irradiance = 32.8 mW cm^{-2}

3 | RESULTS AND DISCUSSION

A typical thiol-ene monomer macroemulsion was prepared by mixing a stoichiometric amount of DAP and DMDS (30.8%w) with an aqueous phase containing a monoacylphosphine oxide lithium salt as radical photoinitiator (TPO-Li) and sodium dodecyl sulfate (SDS) as surfactant (Scheme 2). The interest of using this specific couple of monomers is its long-term storage stability after mixing (Figure S3), whereas problems of spontaneous polymerization are generally encountered in thiol-ene polymerizations.[24] Premature polymerization is thus avoided without the need for additional inhibitor, which could adversely affect the extent of reaction and the polymer MW. The emulsion polymerization starts only when the 385 nm LEDs are switched on. The reaction is carried out at ambient temperature for 60 min and yields a latex with a *z*-average diameter of 163 nm (DLS data). A high conversion (>96%) is achieved within 5 min as proved by ^{1}H NMR spectroscopy, despite a small initiator concentration (0.25%w with respect to the monomers) and a limited radiation penetration within the reactor. A significant increase in temperature from 22 to 49 °C (Figure S4) is observed as a result of the rapid polymerization. However, the thermal control remains manageable, since initiation occurs at ambient temperature and the aqueous continuous phase helps dissipate the heat of polymerization.

3.1 | Molecular weight

We have then conducted a detailed study of the variation of MW throughout the course of the polymerization using SEC. For these measurements, the polymers were isolated by dissolution of samples of the reaction mixture in THF, and accurate MW were obtained by a universal calibration method combining a refractive index (RI) detector (concentration detector) coupled with a viscosity detector to determine the intrinsic viscosity (IV).[25] Note that the calculations of number-average ($\overline{M}_n$) and weight-average MW ($\overline{M}_w$) were started at a mass of approximatively 300 Da, enabling inclusion of all oligomers.[20] Since step polymers may contain a significant fraction of oligomers, such analysis conditions are important for an accurate and correct measurement of MW values and distribution. Figure 2 shows the plot of $\overline{M}_w$ and the MW dispersity ($Đ$) as a function of reaction time. Interestingly, high $\overline{M}_w$ values close to 100,000 Da can be achieved after 20 min of irradiation. After only 5 min of reaction, the MW is larger than 60,000 Da in agreement with the high level of conversion achieved within the first minutes of reaction. This is an important result, since it is generally difficult to achieve very high conversions needed in step polymerization to reach the 10^5-MW range, even for thiol-ene polymerization.[26–28] In chain polymerization, it is generally accepted that the MW of chain polymers is an order of magnitude greater than that in a similar homogeneous free-radical polymerization due to segregation of propagating chains in small particles.[1] Our assumption is that similar compartmentalization effect may also take place in a radical step thiol-ene polymerization as evidenced in a recent study carried out in miniemulsion polymerization.[29] Another interesting observation is the gradual broadening of the MW distribution in the course of the reaction. At the end of the

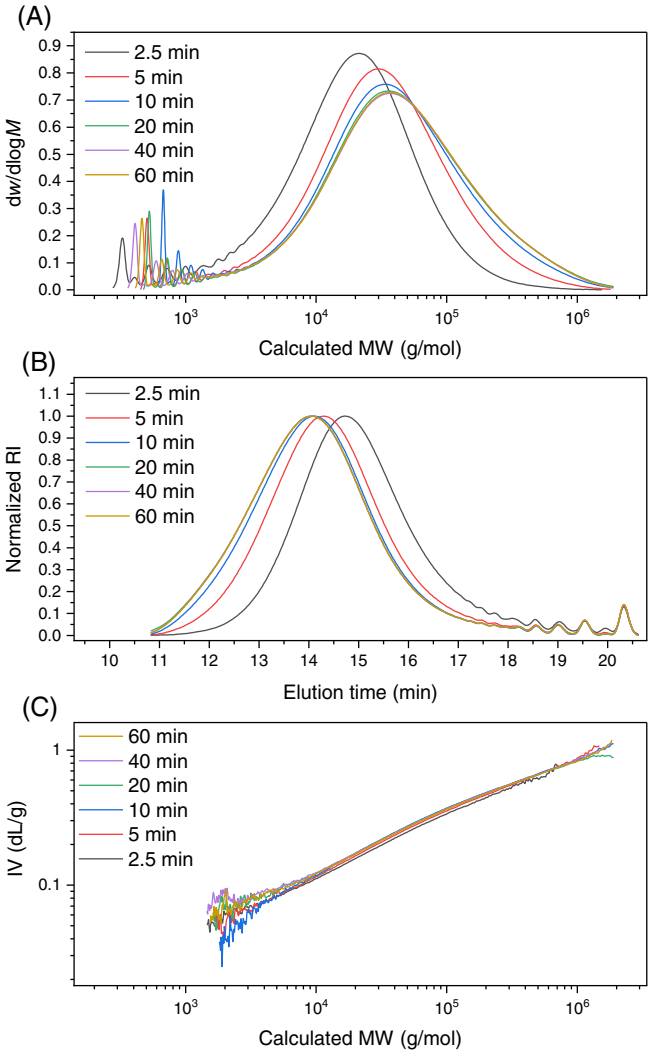

FIGURE 3 (A). d*w*/dLog*M* as a function of calculated polymer MW during diallyl phthalate-2,2′-dimercaptodiethyl sulfide step photopolymerization. This plot gives the distribution function of slice molecular weights with *w* the weight fraction MWD. At low MW range, the variation are experimental errors due to the low sensitivity of the viscosity detector when MW becomes lower than 10^4 Da. (B) Elution profiles obtained with a refractive index detector. (C) Intrinsic viscosity (IV) as a function of molecular weight in the course of the polymerization. Monomer content = 30.8%w (TPO-Li) = 3.73 mM/water, and (SDS) = 30 mM/water, irradiance = 32.8 mW cm^{-2}

polymerization, $Đ$ falls into the range of 9–10, a value indicative of a polymer composed of species of highly differing MW. This stands in marked contrast with the maximum dispersity of two predicted by Flory's theory for a perfectly linear step polymerization excluding cyclization reactions.[30] Therefore, this trend toward strong polymer dispersity at high conversion suggests the competitive formation of cyclic oligomers.[18]

Furthermore, Figure 3A shows a series of weight fraction (*w*) MW distribution obtained with the universal calibration approach for aliquots taken at different irradiation times between 2.5 and 60 min. Regardless of the time, the mass distribution curves are non-uniform with a bimodal shape characteristic of step polymerizations showing a tendency toward cyclization. At low MW, the set of small peaks may be assigned to cyclic oligomers formed by intramolecular cyclization proceeding by the addition of a thiyl radical center on one of the pendant vinyl groups on the same molecule.[31] The broad intense high MW signal shifting toward higher MW with time may contain linear species with possibly a fraction of cyclic species, which is very difficult to evaluate.[32] In contrast, the position of the low MW massif does not seem to change over time, in accordance with the irreversible nature of the cyclization reaction. At the end of the reaction (60 min), the weigh fraction of the low MW species is negligible above 2000 Da and represents 3.2% of the total distribution by weight. Unfortunately, their distribution is not resolved by the viscosity detector used in the universal calibration approach because of their low intrinsic viscosity. Therefore, the noise in the viscosity signal at low MW leads to errors in calculating their weight fraction and molecular weights. Figure 3B shows a series of chromatograms from the RI detector for the same polymerization times. Unsuited to the calculation of accurate MW, the RI detector provides however greater sensitivity to the late eluting low MW peaks in order to assess their evolution through the reaction. Interestingly, the position and intensity of these low MW signals are essentially unchanged in the series of RI chromatograms, whereas the prominent peak shifts toward lower elution time during the polymerization. This clearly supports that the low MW species are dead oligomer species, while the major peak contains a large proportion of linear species increasing continuously in MW by step polymerization. Furthermore, the resolved low-MW peaks in the refractometer chromatograms are roughly observed at 310 ± 76 Da, which is close to the repeat unit mass of the DAP-DMDS dimer (400 Da) (Figure S5). Although the calculated mass values are not correct because they are based on polystyrene calibration,[33] this result is consistent with cyclic species of variable degrees of polymerization (n), ranging predominantly from $n = 1$ for the last eluted peak at 20.3 min (dimer cycle) up to larger rings with $n = 9$ at 17.2 min. The cyclic species formed by reaction between thiol and ene end groups are inert because of the stability of thioether bonds. As a result, cyclic oligomers are able to survive the further course of polymerization, while linear chains continue to grow with increasing conversion. Hence, the difference of $\overline{M}_n$ and $\overline{M}_w$ gradually increases with higher conversion, leading to the observed broadening of the polymer MW.[34]

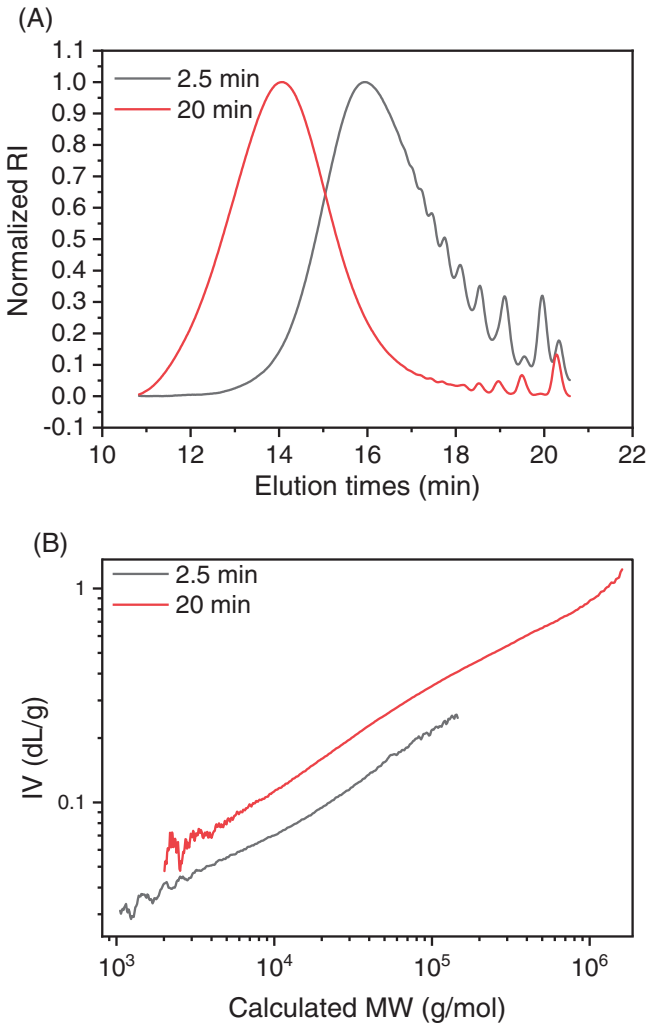

FIGURE 4 Size exclusion chromatography elution curves (RI detector) of polymers collected at 2.5 and 20 min in the course of diallyl phthalate-2,2′-dimercaptodiethyl sulfide emulsion photopolymerization performed at lower irradiance. Intrinsic viscosity (IV) as a function of MW for the same polymers. Monomer content = 30.8%w (TPO-Li) = 3.73 mM/water, and (SDS) = 30 mM/water, irradiance = 6.6 mW cm^{-2}

3.2 | Polymer structure

Although the oligomer species are generally presented as rings in step polymerizations, it is difficult to unequivocally prove this point.[15] In our case, since the coupling thiol-ene reaction is an addition reaction, linear and cyclic species products have exactly the same MW, and are therefore not distinguishable by mass spectrometry techniques.[35] Most of the evidence to support the cyclic nature of these low MW species is therefore indirect, consisting of mechanistic, spectroscopic and SEC data. Firstly, there is no clear evidence of end groups in the ^{1}H NMR and ^{1}C NMR spectra (Figure S6), suggesting that the sample contains only cyclic species and high MW polymer chains in which chain ends are not easily detectable. Secondly, the formation of linear oligomers by deactivation or side reactions of these end group is also unlikely since thiol-ene reaction is known to be tolerant to a variety of functional groups and reaction conditions. Thirdly, we have also attempted to use SEC to assess the presence of different topologies in the same sample. Cyclic polymers have indeed smaller hydrodynamic radius than their linear counterparts of equivalent MW leading to higher retention time and lower intrinsic viscosity.[36] Figure 3C shows an overlay of the Mark-Houwink (M-H) plots of log intrinsic viscosity (IV) as a function of log MW (calculated by the universal calibration method) at different polymerization times. In contrast to our predictions, a similar linear trend can be seen for all samples, suggesting that that the polymers are relatively homogeneous structurally. The MH exponent ranges from 0.42 to 0.53 for the different aliquots, which agrees with a large majority of linear, unbranched, non-crosslinked chains in good solvents.

Our hypothesis is that cyclic oligomers constitute only a too minor proportion of the samples to cause a change in viscosity. We speculated that samples showing lower conversions might be more suited to evidence the presence of rings. To support our assumption, the theory of ring formation predicts that their fraction in cycles is higher in the early stage of the reaction, and decreases rapidly with increasing conversion. This is the result of the reduced kinetic feasibility for cyclization when the ring sizes increase because of lower probability to have two chain ends reacting together.[16] To obtain samples with lower conversions and MW, we have performed the same polymerization with a 5-fold reduction of the irradiance (6.6 instead of 32.8 mW/cm^2) to slow down the polymerization. Figure 4A shows an overlay of the RI chromatograms at 2.5 and 20 min, showing respectively an extent of reaction of 0.88 and 0.97. As expected from a kinetically driven process, the small peaks attributed to cyclic species are more resolved at 2.5 min, and their total weight fraction greater. In addition, the M-H plot at 2.5 min differs markedly from that obtained at 20 min as can be seen in Figure 4B. For equivalent MW, the intrinsic viscosity is substantially lower, agreeing with a higher fraction of cyclic species. Unlike the ratio of η, the M-H exponents (slope) are similar, leading to two relatively parallel lines. This result is expected since the proportion of linear and cyclic species in a sample is known to affect the prefactor K and not the exponent α in the M-H equation[32] $\eta = K \times MW^{\alpha}$. In conclusion, the linear chains seem the most abundant species in a thiol-ene polymerization in emulsion, but cyclic species are present. These latter are preferentially oligomers formed by irreversible intramolecular cyclization in the early stage of the

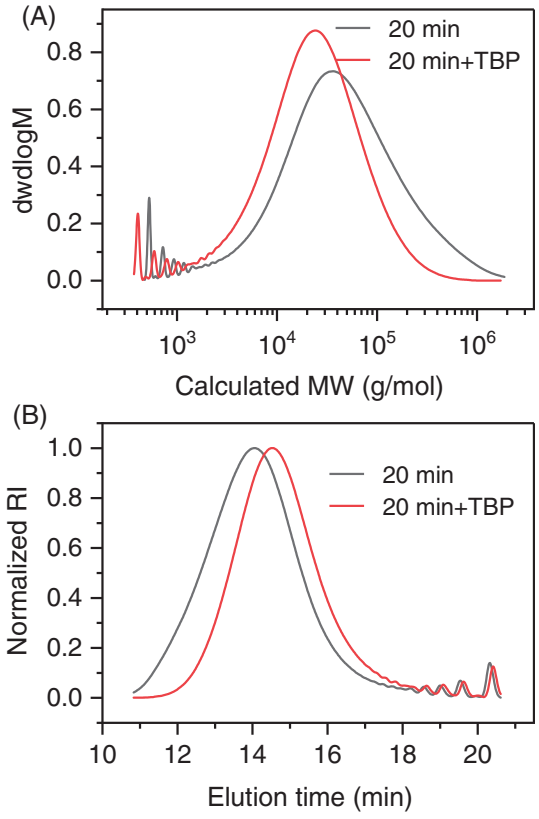

FIGURE 5 (A). Effect of reducing agent tributylphosphine (TBP) on the molecular weight distribution plot of polymer latex obtained after 20 min irradiation. (B) Size exclusion chromatography elution profiles of the corresponding polymers using a RI detector. Monomer content = 30.8%w (TPO-Li) = 3.73 mM/water, and (SDS) = 30 mM/water, irradiance = 32.8 mW cm^{-2}

reaction, as expected from a polymerization proceeding under kinetic control. However, it is possible that the high MW massy contains also a fraction of large rings although their characterization remains difficult.

3.3 | Polymer composition

Another issue is to study the composition of the emulsion polymers. ^{1}H NMR analysis (Figure S6) confirms that the polymer backbone has the expected repeating structure containing thioether bonds (CH_2-S), without visible chain ends. The $\overline{M}_w$ close to 10^5 may be too high to make possible end group detection. However, very small amount of disulfide bonds (<1.2% compared to thioether bonds) can be detected in the ^{1}H-NMR spectra through the disulfide-adjacent methylene protons (-S-S-CH_2-CH_2) arising at 2.85 ppm. The formation of SS bonds probably results from thiyl radical terminated chain ends undergoing recombination reaction (bimolecular termination reaction) instead of the conventional addition across an alkene bond to form a carbon center radical.[37] Due to its low probability, this side reaction has a limited effect on the overall polymer composition which seems to be highly regular. However, the inclusion of even few disulfide bonds has important consequences on the polymer's stability due to the possibility for disulfide bonds to be cleaved in a reducing environment to generate thiols.[38] We have used thiol/disulfide reversibility to induce a controlled chain fragmentation in solution. Figure 5A shows the change of the SEC distribution plot after addition of a large excess of tributylphosphine with respect to the disulfide bond. A substantial reduction of the MW was obtained with a decrease of $\overline{M}_w$ from 99,200 to 39,600 Da as well as a narrowing of MW dispersity from 8.5 to 4.8. Given the low occurrence of disulfide bonds formation within the polymer, the degradation is not complete. The RI chromatogram in Figure 5B shows that the low MW cyclic species are not affected (position, intensity) by the reducing agent, in line with the fact they do not contain any SS bonds. This result is consistent with a lower probability of thiyl radical coupling with decreasing MW. The low MW rings are therefore composed almost exclusively of thioether repeating units (CH_2-CH_2-S-) and can be considered as chemically inert. We have observed a slow decrease of MW during long-term storage that was attributed to chain fragmentation by disulfide reduction (Figure S7). However, steady values of MW, even after 2 months, can be maintained when a water-soluble radical inhibitor (pyrogallol, 1 mM) and a pH buffer (sodium bicarbonate, 10 mM) are added to the latex after preparation (Figure S7). Experiments are underway to find conditions allowing the long-term storage of poly(thioether) latexes without change of MW and particle size.

3.4 | Molecular weight control

Finally, efforts were made to control MW by varying the photoinitiator concentration and the monomer content (Table 1). Figure 6 shows the effect of the monomer content on $\overline{M}_w$ and $Đ$, taking the polymer with a solids content of 30.8%w as benchmark: $\overline{M}_w$ = 99,200 Da, $Đ$ = 8.5 (entry 1, Table 1). Upon decreasing the monomer content to 10%w (entry 2, Table 1), high-MW polymers are produced much more rapidly, typically within 5 versus 20 min previously. A possible explanation may involve higher polymerization rates when decreasing the ratio of monomer to initiator. However, the $\overline{M}_w$ value is unchanged at the end of polymerization. A stronger MW dispersity is observed ($Đ$ = 12.5), presumably because of the formation of a higher fraction of low MW cyclic species since diluted conditions are known to increase the

TABLE 1 Influence of monomer phase content and photoinitiator concentration on final properties of latex produced by diallyl phthalate-2,2′-dimercaptodiethyl sulfide emulsion polymerization

Entry	Monomer phase content (%)	TPO-Li (mM/water)	$\overline{M}_n$ (kDa)	$\overline{M}_w$ (kDa)	$Đ$
1	**30.8**	**3.73**	**11.7**	**99.2**	**8.5**
2	10.0	3.73	7.8	97.2	12.5
3	40.5	3.73	6.2	31.7	5.1
5	10	1.87	9.3	57.3	6.2
6	10	0.93	7.8	40.7	5.2

Note: The data correspond to a similar irradiation time of 20 min.

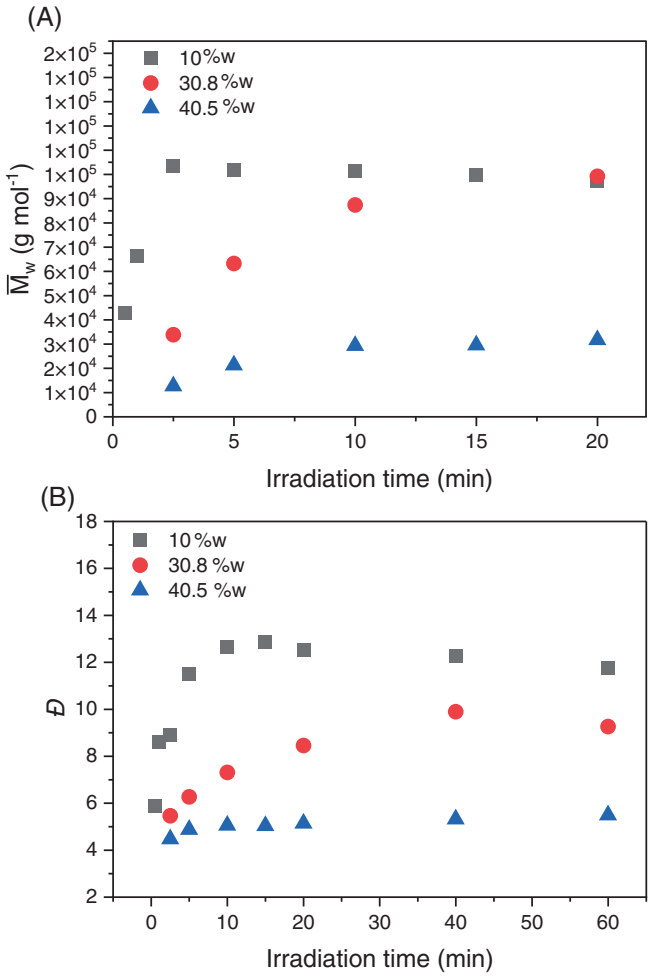

FIGURE 6 Effect of monomer phase content (10–40%w) on polymer MW (A) and molecular weight dispersity $Đ$ (B) during emulsion photopolymerization of 2,2′-dimercaptodiethyl sulfide with diallyl phthalate (SDS) = 30 mM/water, (TPO-Li) = 3.73 mM/water, irradiance = 32.8 mW cm^{-2}

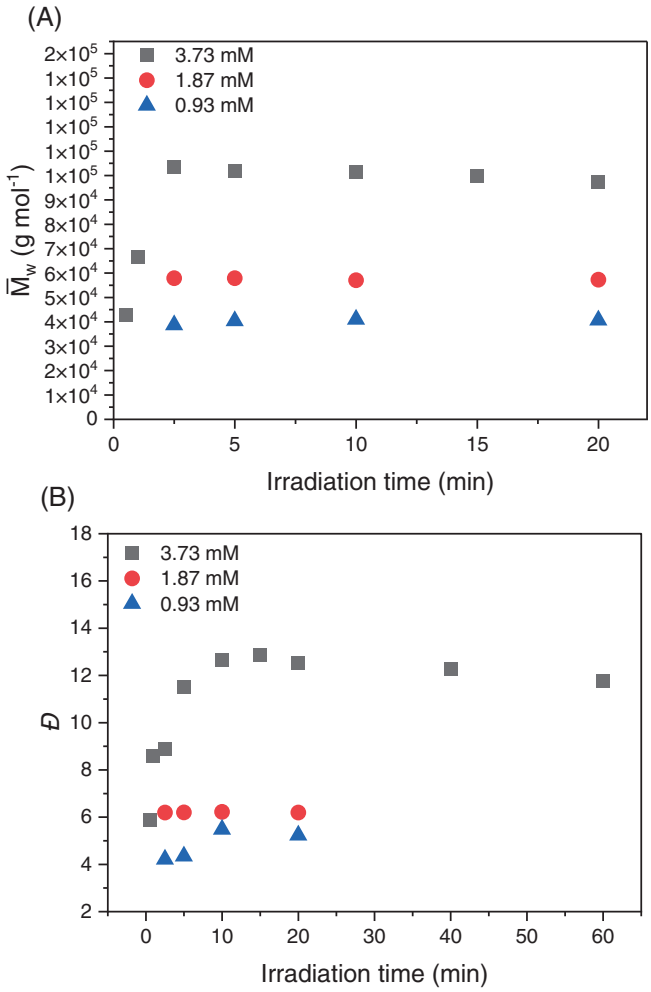

FIGURE 7 Effect of photoinitiator concentration (0.93–3.73 mM/water) on polymer molecular weight (MW) (A) and MW dispersity $Đ$ (B) during emulsion photopolymerization of 2,2′-dimercaptodiethyl sulfide with diallyl phthalate. Monomer phase content = 10%w (SDS) = 30 mM/water, irradiance = 32.8 mW cm^{-2}

cyclization rate.[18] A larger proportion of cycles decreases the value of $\overline{M}_n$, with the consequent effect of increasing the width of the distribution curve. At a monomer phase content of 40.5%w (entry 3, Table 1), there is a significant drop in MW ($\overline{M}_w$ = 31,700 Da) due to the difficulty to achieve very high conversions. Because of the smaller discrepancy in MW values between linear and cyclic species, a narrower MW distribution is obtained ($Đ$ = 5.1).

The effect of the photoinitiator concentration, which is shown in Figure 7, is representative of the strong

impact of conversion on the MW of linear species. $\overline{M}_w$ decreases markedly with the gradual reduction of the initiator concentration from 3.7 to 1.87 mM (entry 4, Table 1), then 0.93 mM (entry 5, Table 1) due to decreasing extent of reaction. The result is a smaller difference between the MW of the linear chains and that of the cyclic oligomers. Therefore, the difference in the number- and weight-average MW is smaller, leading to narrowing of the MW distribution.

4 | CONCLUSION

A photochemical stirred-tank reactor has been used to perform the thiol-step photopolymerization of a bicomponent aqueous emulsion based on 2,2′-dimercaptodiethyl sulfide and diallyl phthalate. The photolatency of this specific thiol-ene mixture is useful to obviate the usage of radical inhibitor generally considered as necessary to avoid spontaneous and uncontrolled polymerization. The resulting latex has a solids content of 30%w and a high $\overline{M}_w$ value close to 100,000 Da as determined by universal calibration method. Such values are rare for step linear polymerizations. A detailed GPC investigation shows a significant molecular weight broadening during the polymerization due to the coexistence of cyclic oligomers and high MW linear chains. Cyclization proceeds by intramolecular addition of a thiyl radical on unsaturated end group in the same molecule and competes with linear polymerization. The formation of stable and low MW rings is a key event to explain the strong dispersity found in emulsion thiol-ene polymerization. The linear chains have a highly regular poly(thioether) structure with some minor inclusions of disulfide units due to thiyl radicals' coupling occurring as side reaction. Their concentration is too small to be measured accurately. However, their presence can be evidenced indirectly by the chain fragmentation induced after the addition of the reducing agent tributylphosphine. The MW of the cyclic oligomers is not affected, meaning that they are devoid of SS bonds and composed exclusively of thioether units. Further effort should be made on understanding the place of cyclization relative to linear polymerization, and its consequences on MW evolution and distribution. Determining how the nature of the thiol and ene monomers affects the competition between cyclization and linear polymerization will be a point of particular interest for future studies.

ACKNOWLEDGMENTS

This project has received funding from the European Union's Horizon 2020 research and innovation programme under the Marie Skłodowska-Curie grant agreement no. 765341 (Project PHOTO-EMULSION, MSCA-ITN-2017). We would like to acknowledge Alexander Peschl (Peschl Ultraviolet GmbH) and Prof. André M. Braun (Karlsruhe Institute of Technology) for their assistance in the design of the stirred-tank photochemical reactor. We are also grateful to Dr. Jean-Luc Birbaum (retired scientist at BASF-Schweiz) for proofreading this document.

CONFLICT OF INTEREST

The authors declare no conflict of interest.

DATA AVAILABILITY STATEMENT

No data availability for this paper.

ORCID

Abraham Chemtob https://orcid.org/0000-0003-4434-1870

REFERENCES

[1] P. A. Lovell, F. J. Schork, *Biomacromolecules* **2020**, *21*, 4396.
[2] J. B. Jönsson, M. Müllner, L. Piculell, O. J. Karlsson, *Macromolecules* **2013**, *46*, 9104.
[3] A. Takasu, A. Takemoto, T. Hirabayashi, *Biomacromolecules* **2006**, *7*, 6.
[4] H. Tanaka, T. Kurihashi, *Polym. J.* **2003**, *35*, 359.
[5] J. C. Saam, D. J. Huebner, *J. Polym. Sci. Polym. Chem. Ed.* **1982**, *20*, 3351.
[6] O. Z. Durham, D. V. Chapman, S. Krishnan, D. A. Shipp, *Macromolecules* **2017**, *50*, 775.
[7] O. Z. Durham, D. A. Shipp, *Polym. Rev.* **2020**, *0*, 1.
[8] C. Quoc Le, M. Schmutz, A. Chemtob, *Macromolecules* **2020**, *53*, 2369.
[9] C. Lowe, C. Bowman, *Thiol-X Chemistries in Polymer and Materials Science*, Royal Society of Chemistry, London, UK **2013**.
[10] C. Resetco, B. Hendriks, N. Badi, F. D. Prez, *Mater. Horiz.* **2017**, *4*, 1041.
[11] T. O. Machado, C. Sayer, P. H. H. Araujo, *Eur. Polym. J.* **2017**, *86*, 200.
[12] Z. Geng, J. J. Shin, Y. Xi, C. J. Hawker, *J. Polym. Sci.* **2021**, *59*, 963.
[13] F. Denes, M. Pichowicz, G. Povie, P. Renaud, *Chem. Rev.* **2014**, *114*, 2587.
[14] C. M. Q. Le, M. Schmutz, A. Chemtob, *Colloid Polym. Sci.* **2022**, *300*, 917. https://doi.org/10.1007/s00396-022-04993-z
[15] M. Uchiyama, M. Osumi, K. Satoh, M. Kamigaito, *Angew. Chem. Int. Ed.* **2020**, *59*, 6832.
[16] G. Odian, *Principles of Polymerization*, John Wiley & Sons, New York **2004**, p. 39.
[17] N. Ballard, J. M. Asua, *Prog. Polym. Sci.* **2018**, *79*, 40.
[18] H. R. Kricheldorf, G. Schwarz, *Macromol. Rapid Commun.* **2003**, *24*, 359.
[19] O. Okay, S. K. Reddy, C. N. Bowman, *Macromolecules* **2005**, *38*, 4501.
[20] H. R. Kricheldorf, S. M. Weidner, F. Scheliga, *Macromol. Symp.* **2017**, *375*, 1600169.
[21] J. M. Asua, in *Polymer Reaction Engineering of Dispersed Systems: Volume II* (Ed: W. Pauer), Springer International Publishing, Cham **2018**, p. 1.

[22] F. Jasinski, P. B. Zetterlund, A. M. Braun, A. Chemtob, *Prog. Polym. Sci.* **2018**, *84*, 47.
[23] T. Majima, W. Schnabel, W. Weber, *Makromol. Chem.* **1991**, *192*, 2307.
[24] C. M. Q. Le, F. Morlet-Savary, A. Chemtob, *Polym. Chem.* **2021**, *12*, 6594.
[25] T. Gruendling, T. Junkers, M. Guilhaus, C. Barner-Kowollik, *Macromol. Chem. Phys.* **2010**, *211*, 520.
[26] J. M. Sarapas, G. N. Tew, *Angew. Chem. Int. Ed.* **2016**, *55*, 15860.
[27] O. van den Berg, T. Dispinar, B. Hommez, F. E. Du Prez, *Eur. Polym. J.* **2013**, *49*, 804.
[28] P.-K. Dannecker, U. Biermann, A. Sink, F. R. Bloesser, J. O. Metzger, M. A. R. Meier, *Macromol. Chem. Phys.* **2019**, *220*, 1800440.
[29] L. Infante Teixeira, K. Landfester, H. Thérien-Aubin, *Polym. Chem.* **2022**, *13*, 2831.
[30] H. Kricheldorf, in *Polycondensation: History and New Results* (Ed: H. Kricheldorf), Springer, Berlin, Heidelberg **2014**, p. 35.
[31] E. M. Scanlan, V. Corcé, A. Malone, *Molecules* **2014**, *19*, 19137.
[32] D. E. Niehaus, C. Jackson, *Polymer* **2000**, *41*, 259.
[33] L. K. Kostanski, D. M. Keller, A. E. Hamielec, *J. Biochem. Biophys. Methods* **2004**, *58*, 159.
[34] S. M. Weidner, H. R. Kricheldorf, F. Scheliga, *J. Polym. Sci. Part A: Polym. Chem* **2016**, *54*, 197.
[35] P. Wessig, T. Schulze, A. Pfennig, M. Weidner, S. Prentzel, H. Schlaad, *Polym. Chem.* **2017**, *8*, 6879.
[36] J. P. Edwards, W. J. Wolf, R. H. Grubbs, *J. Polym. Sci. Part A: Polym. Chem* **2019**, *57*, 228.
[37] E. Q. Rosenthal, J. E. Puskas, C. Wesdemiotis, *Biomacromolecules* **2012**, *13*, 154.
[38] A. Takahashi, R. Goseki, H. Otsuka, *Angew. Chem. Int. Ed.* **2017**, *56*, 2016.

SUPPORTING INFORMATION

Additional supporting information can be found online in the Supporting Information section at the end of this article.

How to cite this article: C. M. Q. Le, A. Chemtob, *J. Polym. Sci.* **2022**, 1. https://doi.org/10.1002/pol.20220402